Published in Physical Review B 57, issue 24, 15251-15260, 1998
which should be used for any reference to this work

Theoretical analysis of the electronic structure of the stable and metastable $c(2\times2)$ phases of Na on Al(001): Comparison with angle-resolved ultraviolet photoemission spectra

C. Stampfl
Xerox Palo Alto Research Center, 3333 Coyote Hill Road, Palo Alto, California 94304

K. Kambe
Prinzregentenstrasse 56/57, D-10715 Berlin, Germany

R. Fasel and P. Aebi
Institut de Physique, Université de Fribourg, Prollés, 1700 Fribourg, Switzerland

M. Scheffler
Fritz-Haber-Institut der Max-Planck-Gesellschaft, Faradayweg 4-6, D-14195 Berlin-Dahlem, Germany

Using Kohn-Sham wave functions and their energy levels obtained by density-functional-theory total-energy calculations, the electronic structure of the two $c(2\times2)$ phases of Na on Al(001) are analyzed, namely, the metastable hollow-site structure formed when adsorption takes place at low temperature, and the stable substitutional structure appearing when the substrate is heated thereafter above 180 K or when adsorption takes place at room temperature from the beginning. The experimentally obtained two-dimensional band structures of the surface states or resonances are well reproduced by the calculations. With the help of charge-density maps, it is found that, in both phases, two pronounced bands appear as the result of a characteristic coupling between the valence-state band of a free $c(2\times2)$-Na monolayer and the surface-state/resonance band of the Al surfaces; that is, the clean (001) surface for the metastable phase and the unstable, reconstructed ''vacancy'' structure for the stable phase. The higher-lying band, being Na derived, remains metallic for the metastable phase, whereas it lies completely above the Fermi level for the stable phase, leading to the formation of a surface-state/resonance band structure resembling the bulk band structure of an ionic crystal.

I. INTRODUCTION

The adsorption of alkali-metal atoms on metal surfaces has attracted much attention in recent years partly due to the discovery of a variety of adsorbate phases, in particular, structures that involve a reconstruction of the metal surface induced by the alkali-metal atoms (see, for example, Refs. 1 and 2, and references therein). A common feature of these systems is that often there is a metastable phase at low temperature involving no reconstruction of the metal surface, while, at higher temperatures, a stable reconstructed phase occurs.

In the present paper we present a combined theoretical and experimental investigation of one such system, namely, that of $c(2\times2)$ phases of Na on Al(001). Early dynamical-theory analyses of low-energy electron-diffraction (LEED) intensities[3,4] concluded that Na occupied the fourfold hollow site. It was first demonstrated by high-resolution core-level spectroscopy[5] and surface extended x-ray-absorption fine-structure (Ref. 6) studies that the hollow site is taken only for preparations at low temperature (LT), and a different, stable structure is formed by adsorption at room temperature (RT) or by heating of the LT phase above c. 160 K. It was shown later by a density-functional theory (DFT) study[7] and by a LEED analysis[8] that in the RT phase the Na atoms occupy substitutional sites, where every second Al atom in the top layer is removed and a Na atom adsorbed in its place. The result of an x-ray photoelectron diffraction (XPD) study[9] of the RT phase concluding that the surface contains two domains, could not be confirmed.[8]

In what follows, we perform a theoretical analysis of the *electronic* structure of the two $c(2\times2)$ structures, and compare the results with those of angle-resolved ultraviolet spectroscopy.[10] The measurements have been performed in what we call ''polar scan'' modes, which deliver displays of photoemission intensities as a function of energy and wave-vector component parallel to the surface, lying in selected symmetry directions ($\bar{\Gamma}$-$\bar{M}$ and $\bar{\Gamma}$-$\bar{X}$) in the two-dimensional (2D) Brillouin zone (see Fig. 1). The displays yield directly 2D band structures of surface states/resonances (i.e., surface states *or* resonances, depending on the position of the states in or out of the gap of the 2D projected bulk bands), which may be compared with calculated results.

The basis of our theoretical analysis are Kohn-Sham wave functions, and their energy levels obtained by DFT total-energy calculations.[7] 2D band structures are derived and compared with the experimental results. The obtained, satisfactory agreement between theory and experiment may be regarded as support of the proposed atomic structure models mentioned above, and a useful basis for further studies of the properties of these surfaces.

Also, single-state charge-density distributions of occupied and unoccupied states are derived from the DFT calculation,

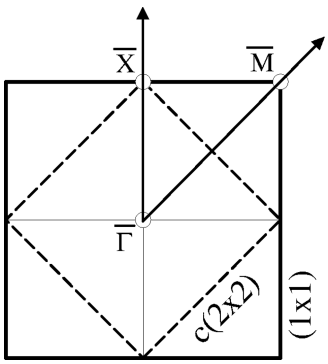

FIG. 1. Surface Brillouin zone of 1×1 (full lines) and $c(2\times2)$ (broken lines) structures. The symmetry points $\overline{\Gamma}$, $\overline{M}$, and $\overline{X}$ refer to the (1×1) structure.

and used for analyzing the character of the bands. We find that adsorption leads, in both LT and RT cases, to *two* main bands of surface state/resonances as the result of a coupling between the valence-state band of a free $c(2\times2)$-Na monolayer and the surface-state/resonance band of the Al surface. Across the Fermi level the Al-derived band is shifted down, and the Na-derived band is shifted up. As a consequence, a charge transfer takes place from the adsorbate directly into the *pre-existent surface state/resonance* of the substrate.

For the LT (hollow) structure, it is found that the coupling is relatively weak and the Al-derived state almost retains the perfect 1×1 periodicity of the clean surface. For the RT (substitutional) structure, the Al-derived state exhibits a clear $c(2\times2)$ periodicity of the reconstructed Al surface. The Na-derived band of the RT structure is completely empty, and leads, except for the still existent background bulk continuum, to a surface electronic structure having a character of an *ionic* monolayer lying on the surface. We discuss possible consequences of this finding.

The paper is organized as follows: In Sec. II, the experimental method is outlined, and is followed in Sec. III by a description of the calculation methods. Section IV contains the results for the surface-state/resonance band structures and the analysis of the character of the bands in terms of single-state charge-density distributions. Also, the charge-transfer processes are analyzed by using density differences. Section V contains the discussion, and Sec. VI the conclusion.

II. EXPERIMENT

The photoemission experiments[10] were performed in a VG ESCALAB Mark II spectrometer modified for motorized sequential angle-scanning data acquisition,[11] and with a working pressure in the lower 10^{-11}-mbar region. Ultraviolet photoelectron spectroscopy measurements were done using unmonochromatized He I (21.2 eV) radiation from a discharge lamp. The 150-mm-radius hemispherical analyzer was run with an energy resolution of 50 meV. Contamination-free surfaces were prepared by a combination of Ar^+ sputtering and annealing at 500 °C. Na was evaporated from a carefully outgassed SAES getter source. Particular care was taken to ensure ultraclean Na deposits: All parts of the evaporation source, except the tiny exit slit, were surrounded with liquid-nitrogen-cooled walls. In this way, the pressure during evaporation could be kept as low as 2.5×10^{-11} mbar. Na coverages were determined accurately (±0.03 ML) from core-level photoelectron intensities.[12] The sample temperature was measured with a thermocouple in mechanical contact with the sample holder. The temperature gradient between the sample and the sample holder was determined in a separate calibration experiment with an additional thermocouple spot welded onto a dummy sample. Sample temperatures given here are corrected for this temperature difference and are estimated to be correct within ±10 K.

In order to obtain two-dimensional band structures of surface states/resonances, polar scans along the $\overline{\Gamma}$-$\overline{M}$ and $\overline{\Gamma}$-$\overline{X}$ directions of the Al(001) surface Brillouin zone were performed, recording at each angular setting ($\Delta\Theta=2°$) the entire photoelectron spectrum between -0.4- and 4.3-eV binding energy. The experimental data sets $I(E_i,\Theta)$ acquired in this way were mapped onto a regular $(E_i,\mathbf{k}_\parallel)$ grid, and visualized as gray-scale plots with low intensities in white and high intensities in black.

III. CALCULATION METHOD

The *ab initio* DFT total-energy calculations, and comparison with LEED results are described in Refs. 7 and 8. The calculations were performed using the local-density approximation (LDA) for the exchange-correlation functional. Further details about the method can be found in Refs. 7,13 and 14. The following two kinds of diagrams have been used in the present analysis.

(1) *2D band structures*. For deriving 2D band structures we use the following procedure. The projected density of states (DOS) onto a chosen atomic orbital $\psi_{\mathrm{AO}}(\mathbf{r})$ is defined as

$$N_{\mathrm{AO}}(\varepsilon)=\sum_{\mathbf{k}_\parallel} N_{\mathrm{AO}}(\mathbf{k}_\parallel,\varepsilon), \tag{1}$$

where the ''$\mathbf{k}_\parallel$-resolved'' projected DOS is given by

$$N_{\mathrm{AO}}(\mathbf{k}_\parallel,\varepsilon)=\sum_{\varepsilon'}\left|\int_{r<r_c} d^3\mathbf{r}\ \psi^*_{\mathrm{AO}}(\mathbf{r})\,\psi_{\mathbf{k}_\parallel,\varepsilon'}(\mathbf{r})\right|^2$$

$$\times\frac{\gamma}{\pi}\frac{1}{(\varepsilon'-\varepsilon)^2+\gamma^2}. \tag{2}$$

For $\psi_{\mathrm{AO}}(\mathbf{r})$, we have used the eigenfunctions of the isolated pseudoatoms from which the pseudopotentials were derived for the total-energy calculation.[7] The integral was truncated at a cutoff radius r_c. (Here we used $r_c=3.7$ Å.) In the standard supercell method using a slab geometry, a Kohn-Sham state $\psi_{\mathbf{k}_\parallel,\varepsilon}(\mathbf{r})$ can be specified, except for the presence of degeneracy, by indices $\mathbf{k}_\parallel$ and ε (both discrete), the parallel wave vector, and the energy, respectively. The lifetime broadening parameter γ is introduced for convenience in numerical work and for improving visibility of peaks in the resulting plots. (Here we take $\gamma=0.5$ eV.)

A simple sum of $N_{\mathrm{AO}}(\mathbf{k}_\parallel,\varepsilon)$'s are formed over atomic orbitals of a specified atom. For example, for Na, we have

TABLE I. Legends of the symbols used in calculated 2D band structures in Figs. 2 and 3. The ''minimum fraction'' is defined in the text (the calculation method in Sec. III).

Structure	Symbol	Projected atom	Min. fraction $\overline{\Gamma}$-$\overline{X}$	Min. fraction $\overline{\Gamma}$-$\overline{M}$
clean	big circles	Al	0.8	0.8
	small circles	Al	0.4	0.4
LT	empty squares	Na	0.5	0.5
	big circles	Al	0.7	0.8
	small circles	Al	0.35	0.4
RT	big squares	Na	0.4	0.5
	small squares	Na	0.2	0.2
	small circles	Al	0.5	0.55
vacancy	big circles	Al	0.5	0.5
	small circles	Al	0.3	0.3

$$N_{\mathrm{Na}}(\mathbf{k}_{\parallel},\varepsilon)=N_{\mathrm{Na}3s}(\mathbf{k}_{\parallel},\varepsilon)+N_{\mathrm{Na}3p_x}(\mathbf{k}_{\parallel},\varepsilon)+N_{\mathrm{Na}3p_y}(\mathbf{k}_{\parallel},\varepsilon)+N_{\mathrm{Na}3p_z}(\mathbf{k}_{\parallel},\varepsilon). \quad (3)$$

The corresponding quantities $N_{\mathrm{Al}}(\mathbf{k}_{\parallel},\varepsilon)$ are evaluated for the Al atoms in the uppermost layer. The maximum peak of these quantities was always found at the bottom of a surface-state/resonance band lying at $\overline{\Gamma}$. Those peaks having a fractional ratio to the maximum higher than a properly chosen fixed value (''Min. Fraction'' in Table I), are selected and their positions in $(\mathbf{k}_{\parallel},\varepsilon)$ space displayed, using squares for Na and circles for Al (see Table I). The plots along $\overline{X}$-$\overline{\Gamma}$ and $\overline{\Gamma}$-$\overline{M}$ (see Fig. 1) are combined, and are presented in Figs. 2 and 3. We see that they produce satisfactorily 2D band structures to be compared to the experimentally obtained ones.

The bulk-band continuum is separated into discrete bands due to the use of finite (nine layer) Al slabs. They appear in Figs. 2 and 3 as weak features. The discreteness of bulk bands may have caused a small energy shift of the surface *resonance* bands lying inside the bulk continuum, because these are replaced by one of the discrete bulk bands lying nearest to them.

We note that in Figs. 2 and 3 the theoretical bands for the LT and RT structures repeat themselves inside the 1×1 Brillouin zone, exhibiting $c(2\times2)$ periodicity. That is, the range $\overline{\Gamma}$-$\overline{M}$ [$\overline{M}$ refering to (1×1)] is halved, and the bands in the second half become a mirror image of the first half. We call this ''backfolding'' here (cf. Ref. 15). It is a consequence of our use of the density of states projected to one specified atom in each $c(2\times2)$ surface unit cell. We note that this is obviously a theoretical construct, and not quite adequate for fully representing the character of the wave functions of the bands, particularly in the LT structure. In fact, there is no information included about the relation between the values of wave functions around the two Al atoms in a unit cell (see Fig. 4). Thus, in reality the wave functions may happen to have approximately a 1×1 Bloch-type periodicity—the backfolding still occurs. The same would also result even for the clean-surface band if the artificial $c(2\times2)$ unit cell would be imposed. In our backfolded band structure, a vanishing deviation from the 1×1 Bloch-type periodicity would become visible only in a vanishing band gap at a Brillouin-zone boundary, that is, in our case on the line halving the range $\overline{\Gamma}$-$\overline{M}$.

On the other hand, the photoemission intensity would be determined by a matrix element

$$M(\mathbf{k}_{\parallel},\varepsilon)=\int d^3\mathbf{r}\ \psi_{\mathrm{f}}^{*}(\mathbf{r})\nabla\psi_{\mathbf{k}_{\parallel},\varepsilon'}(\mathbf{r}). \quad (4)$$

The symmetry of the structure leads to the ''selection rule,'' which selects out initial-state bands according to the symmetry relation between the initial- and final-state wave functions. In the case of the LT structure, the final state $\psi_f(\mathbf{r})$ samples the initial state $\psi_{\mathbf{k}_{\parallel},\varepsilon'}(\mathbf{r})$ at both of the two Al atoms in a unit cell. The selection rule can take place differently for the first and second halves of the range $\overline{\Gamma}$-$\overline{M}$, destroying the mirror symmetry between the two halves. In particular, if the wave functions have nearly the 1×1 Bloch-type periodicity, the selection rule leads to an ''unfolding'' of the backfolded band structure.

(2) *Charge-density distributions*. The charge density is derived from Kohn-Sham wave functions as

$$\rho(\mathbf{r})=\sum_{\mathbf{k}_{\parallel}}\sum_{\varepsilon\ \mathrm{occ}}|\psi_{\mathbf{k}_{\parallel},\varepsilon}(\mathbf{r})|^2, \quad (5)$$

where ε occ labels the occupied levels. We use $\rho(\mathbf{r})$ for the study of charge transfer occurring at adsorption.

The single-state charge density is defined here as

$$\rho_{\mathbf{k}_{\parallel},\varepsilon}(\mathbf{r})=|\psi_{\mathbf{k}_{\parallel},\varepsilon}(\mathbf{r})|^2, \quad (6)$$

and used for analyzing the character of surface states/resonances. We should keep in mind that the charge-density distributions are derived from *pseudo*-wave-functions resulting from the use of pseudopotentials, so that they give a correct distribution only outside the critical radius of the pseudopotentials.

We use cross sections of the charge densities on planes perpendicular and parallel to the surface. The perpendicular cross sections taken are specified in Fig. 4.

IV. RESULTS

In Secs. IV A, IV B, and IV C, we discuss successively the results for the clean Al(001) and the two $c(2\times2)$-Na/Al(001) surfaces. It is to be noted that the figures are arranged, independently of the text, in the way to facilitate a visual comparison between the different structures.

A. Clean Al(001)

Figure 2(a) shows the experimental (left panel) and theoretical (right panel) band structures for the clean Al(001) surface. It can be seen that both exhibit a surface-state band

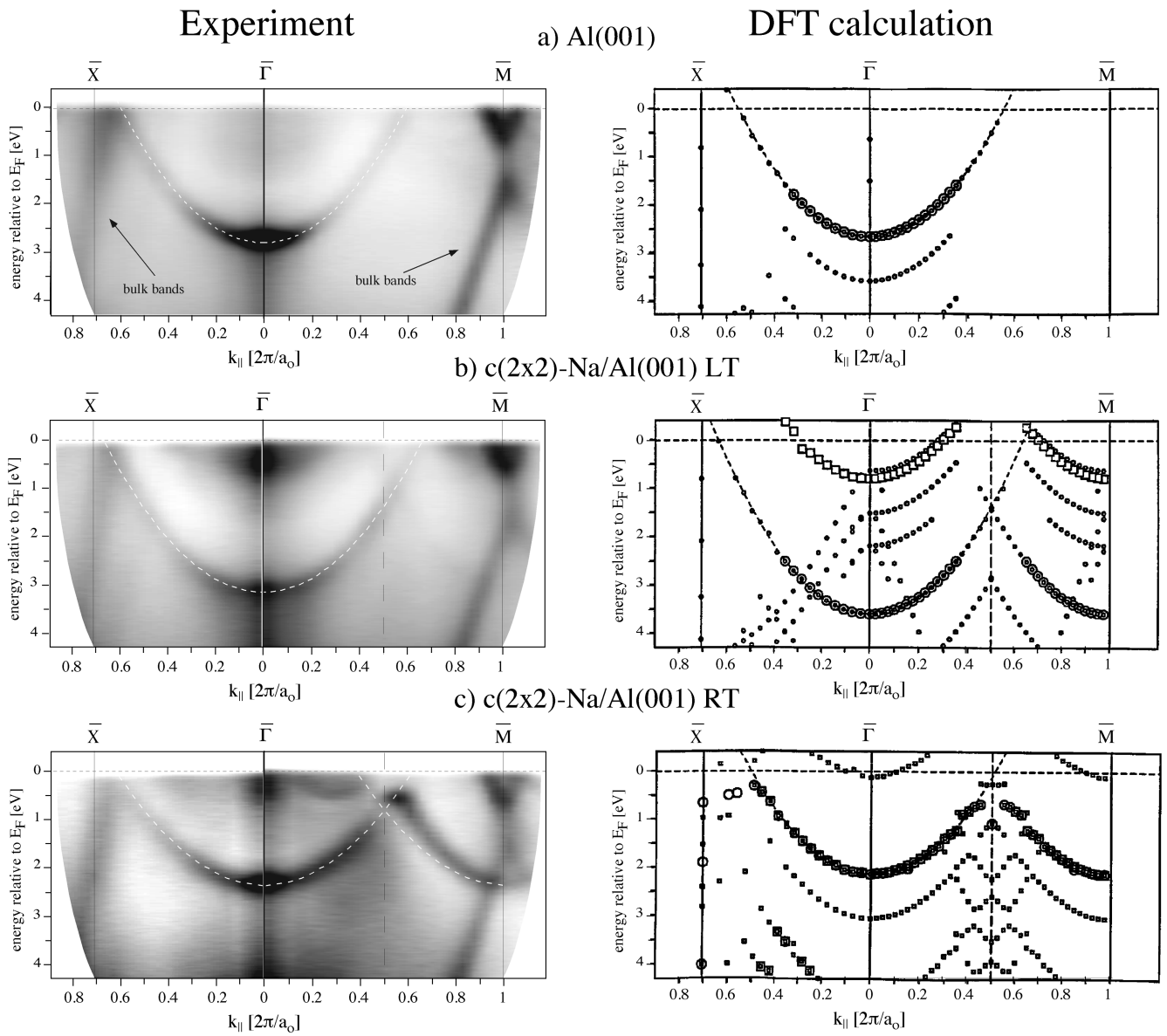

FIG. 2. Comparison of experimental (left panel) and calculated (right panel) 2D band structures. The symbols used for the calculated bands are specified in Table I. (a) Clean surface. (b) LT phase (hollow site). (c) RT phase (substitutional site).

which has a free-electron-like form. The paramaters obtained by fitting by parabolas, as indicated by broken lines in Fig. 2(a), are shown in Table II. The energy position of the band at $\overline{\Gamma}$, E_0, agrees well between theory and experiment, with values of 2.68 and 2.76 eV below the Fermi level, respectively. The theoretical value lies in the range of the results of other calculations:[16–23] 2.6–2.9 eV. The experimental value is in very good agreement with earlier experimental studies.[24–26]

In Fig. 2 (left panel), it can be seen that the experimental results display a number of additional features. Those which are common to all structures studied on this surface are assigned to bulk bands, as indicated by arrows. These bulk features do not appear in the calculated band structures (right panel), reflecting the fact that the density of states projected onto the uppermost Al atoms are dominated by the surface states.

In Fig. 6(a) we display the single-state charge-density distributions at $\overline{\Gamma}$ for the main band. The two cross sections (100) and (110) are defined in Fig. 4(a). An important characteristic of the surface state of the clean Al(001) surface is that the charge density shows a pronounced maximum just on top of the surface Al atoms. This can also be seen in the cross section parallel to the surface through the electron-density maxima as shown in Fig. 7(a). This particular feature of the surface state is apparently crucial in the formation of the electronic structure of the LT phase, as we see below.

B. LT $c(2\times2)$ hollow structure

1. Al-derived band

In Fig. 2(b), we show the experimental (left panel) and calculated (right panel) surface states/resonances for the LT $c(2\times2)$ hollow structure. The lower-lying main band is Al derived, as indicated by the circles in the theoretical plot (cf. Table I). The position of the calculated band at $\overline{\Gamma}$ lies somewhat lower in energy than the experimental value; compare 3.61 to 3.12 eV (see Table II). (We note the calculated re-

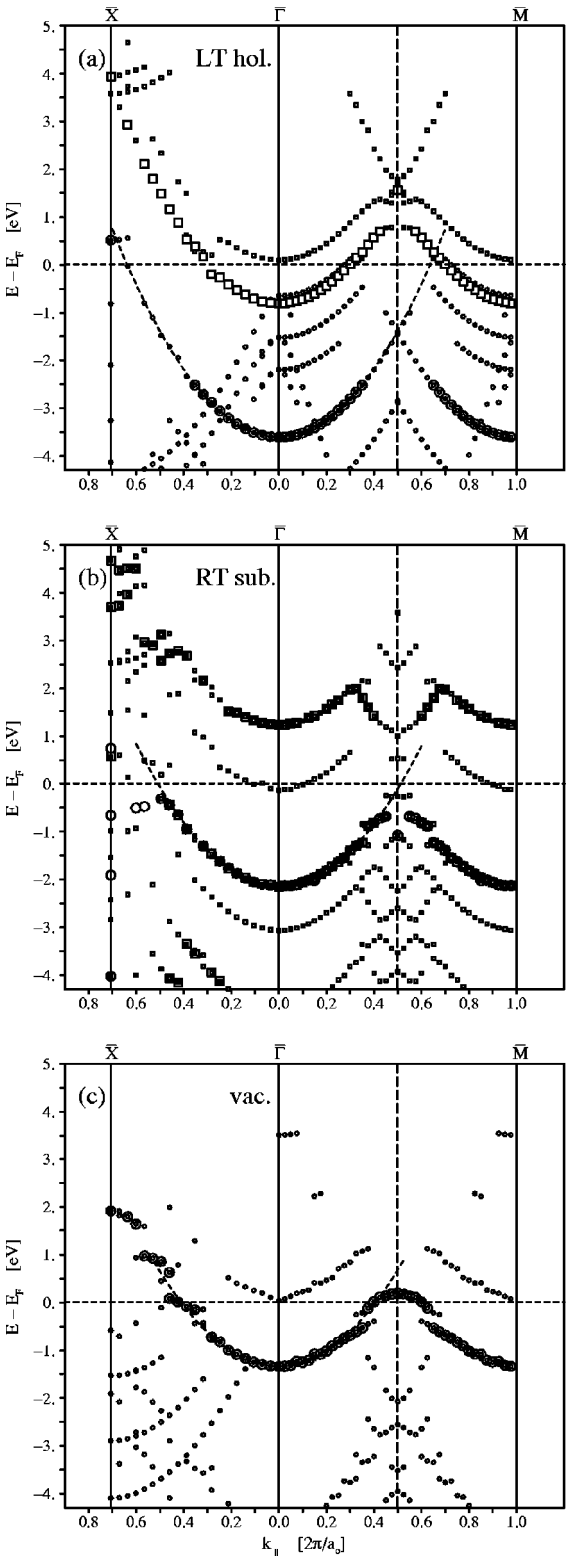

FIG. 3. 2D band structures of (a) the LT phase (hollow site), (b) the RT phase (substitutional site), and (c) the vacancy structure, including the energy range above E_F. The symbols used are specified in Table I.

sults of the earlier theoretical work of Chulkov and Silkin[18] is also ≈3.6 eV, although their non-self-consistent value of vertical distance 2.05 Å, from Na to Al is different from ours 2.35 Å, which is nearer to the experimental result 2.57 A.[8]) Compared to the position of the surface-state band of the

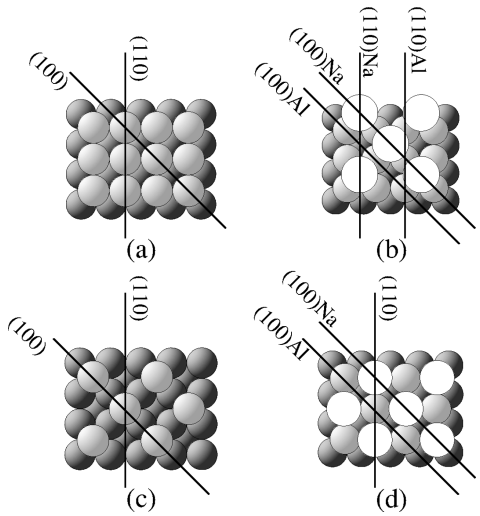

FIG. 4. Geometries of the $c(2\times2)$-Na/Al(001) surface structures: (a) clean surface (b) LT phase (hollow site), (c) vacancy structure, and (d) RT phase (substitutional site). The positions of perpendicular cross sections used for charge-density distributions are indicated. The white circles represent Na atoms, and the gray circles Al atoms.

clean Al(001) surface, the Al-derived band lies lower in energy, by 0.93 and 0.36 eV, as obtained by the calculations and as determined from experiment, respectively. The nature of this downward shift will be discussed below. The differences between theory and experiment may have been caused by the approximations used in the total-energy calculation (use of LDA, Rydberg cut, k-point sampling, etc.[13,14])

The experimental results show clearly that the Al-derived state does *not* have the $c(2\times2)$ periodicity, but rather the 1×1 periodicity of the clean surface. In fact, we find it a significant experimental result that the main band in the LT phase has, throughout the whole range of $\bar{\Gamma}$-$\bar{M}$, almost the same form as that of the clean surface, being only shifted down.

In Fig. 6(b) we display the single-state charge-density distribution at $\bar{\Gamma}$ for the Al-derived band of the LT phase. The two sets of cross sections differently chosen for Al and Na [cf. Fig. 6(c)] are defined in Fig. 4(b). It can be noted in Fig. 6(b) that the maxima of charge density remains on top of the surface Al atoms, almost unchanged from those of the clean surface shown in Fig. 6(a). (This has also been pointed out by Chulkov and Silkin.[18]) In the cross section parallel to the surface shown in Fig. 7(b), only a small deviation from the 1×1 structure is seen, having a $c(2\times2)$ period, with some indication of a character of a bonding state between the Na

TABLE II. Parameters specifying the main surface state/ resonance bands in Figs. 2 and 3. The experimental values (Ref. 10) are shown in brackets.

Structure	E_0 (eV)	k_F $[2\pi/a_0]$	m^* (m_e)
clean	2.68 (2.76)	0.55 (0.60)	1.05 (1.18)
LT	3.61 (3.12)	0.64 (0.66)	1.03 (1.29)
RT	2.14 (2.31)	0.51 (0.62)	1.12 (1.55)
vacancy	1.33	0.41	1.15

and Al atoms. The smallness of the deviation explains the similarity of the experimental band structures between the clean surface and the LT phase. It is to be noted that in the photoemission processes from this band, not only the initial states, but also the final states, have apparently maintained approximately the same periodicity as of the clean surface. The theoretical curves in Fig. 2(b) appear different, but this is only caused by the backfolding, as already mentioned.

2. Na-derived band

In Fig. 2(b), dark spots can be seen at $\bar{\Gamma}$ and $\bar{M}$, near the Fermi energy E_F, in the experimental results. Although from the figure presented here it is perhaps difficult to distinguish, we find in the experimental data that the dark feature at $\bar{M}$ for the LT phase is markedly different in character from that of the clean surface, in that the intensity for the LT phase is stronger and some tailing with dispersion is exhibited, as is the case also for the feature at $\bar{\Gamma}$. From the calculated bands of the LT phase [right panel of Fig. 2(b)], we can see that there is a surface-state/resonance band with an energy of about 0.7 eV below the Fermi level at $\bar{\Gamma}$. As indicated by the open squares, it is a Na-derived band. We assign this band as giving rise to the experimentally measured intensities at $\bar{\Gamma}$ and $\bar{M}$ at $\sim$0.4 eV below the Fermi level. The existence of this band was first theoretically predicted by Benesh *et al.*,[27] and was also reproduced by Chulkov and Silkin.[18] In Fig. 3(a), we show the same calculated band structure as in Fig. 2(b), but where the energy region extends higher into the positive range. Here we can see that the part of the Na-derived band above E_F exhibits marked band-structure effects in the middle of $\bar{\Gamma}$-$\bar{M}$, due to the $c(2\times2)$ periodicity of the adsorbed Na layer.

In Fig. 5(a), we show the band structure of a free $c(2\times2)$-Na monolayer for comparison. It can be observed that at $\bar{\Gamma}$ the lowest band lies $\approx$0.8 eV lower in energy as compared to the Na-derived band of the LT phase. Correspondingly the occupied part of the band is notably larger for the free monolayer.

Figure 6(c) displays the distribution of the Na-derived surface state/resonance at $\bar{\Gamma}$ which clearly shows an antibonding character, the nodal line (not shown) running between the Na and Al layers. A comparison with Fig. 5(b) shows that the strongly smeared out character of the density between the Na atoms is maintained, appearing, however, only in the upper half of the Na layer. The lower half is apparently canceled by the Al surface states due to the antibonding coupling. A cross section parallel to the surface passing through the electron density maxima on top of the Na atoms is shown in Fig. 7(c). Here we see also a smeared out, free-electron-like distribution.

3. Formation mechanism of the two surface-state/resonance bands

Combining the results above, we can conclude that the two bands are resulting from a coupling between the lowest-lying (3*s*-derived) band of a free $c(2\times2)$ monolayer of Na and the surface-state band of the clean Al(001) surface. Applying a simple two-term perturbation theory, as commonly done in molecular-orbital theory,[28,29] this may be understood as being due to the formation of bonding and antibonding states, leading to the downward shift of the Al-derived band by 0.9 eV (calc.), with an increase in population and the upward shift of the Na-derived band by 0.8 eV (calc.) with a decrease in population. Alternatively, it may be understood, as in the case of ionic crystals, that the shifts occur as the result of Coulomb fields between the two oppositely charged ionic layers. The ionization is to be expected due to the cationic nature of Na, which donates electronic charge to the aluminum.

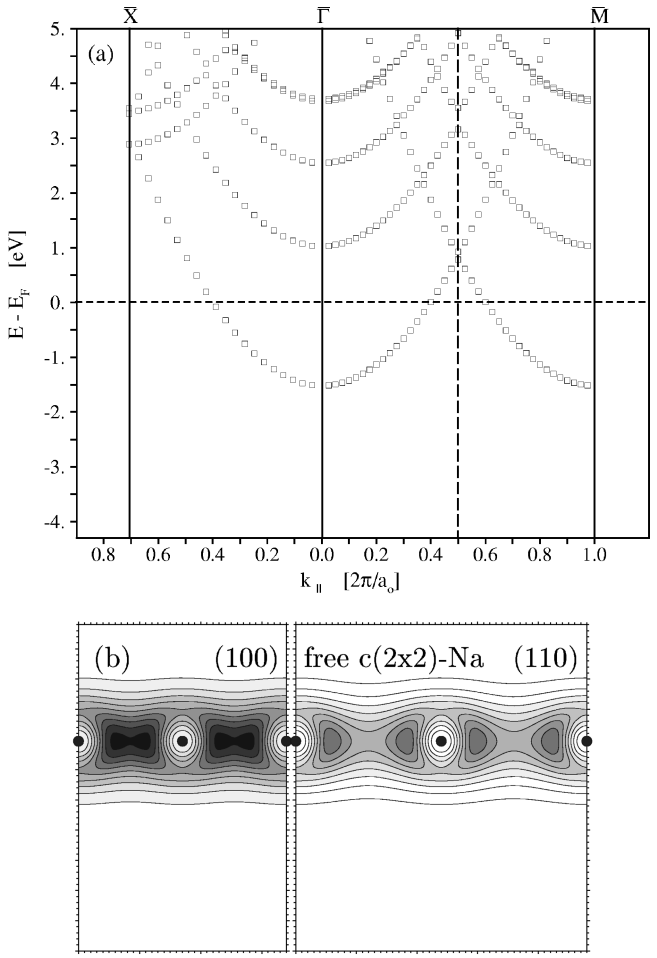

FIG. 5. Free $c(2\times2)$-Na layer: (a) band structure, and (b) charge-density distribution of valence elctrons. The planes of cross sections are defined in Fig. 4(b).

In Fig. 9, we show the total charge density $\rho_{\text{tot.}}$; the density difference between the adsorption system and the corresponding Al surface (for which the positions of the Al atoms are kept at those of the adsorption system), $\Delta\rho_{\text{diff.}}=\rho_{\text{tot.}}-\rho_{\text{Al}}$, and the *redistribution* of charge, $\Delta\rho_{\text{redis.}}=\rho_{\text{tot.}}-\rho_{\text{Al}}-\rho_{\text{c(2}\times\text{2)-Na}}$, which subtracts out the charge density of the free Na monolayer [Fig. 5(b)], showing exactly where charge has been enhanced and depleted. It can clearly be seen from $\Delta\rho_{\text{diff.}}$ and $\Delta\rho_{\text{redis.}}$ that charge enhancement occurs primarily at the maxima of the surface states, and indeed almost proportionally. We can also note in $\Delta\rho_{\text{redis.}}$ some regions of depletion, showing that the electron charge has been transferred from the upper half of the region between the Na

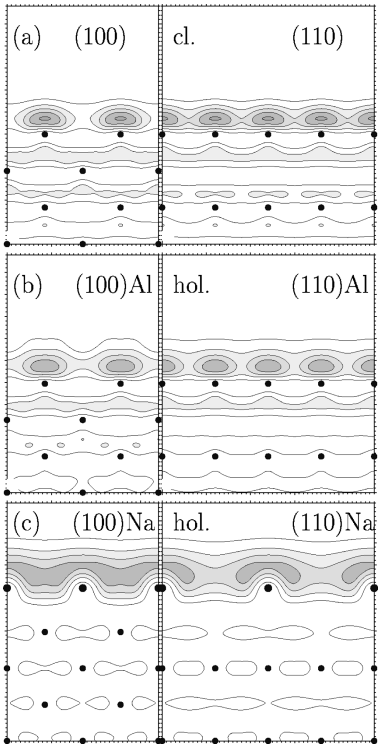

FIG. 6. Charge-density distribution of the surface state/resonance of the main bands at $\bar{\Gamma}$ for (a) the clean surface, (b) the Al-derived band of the LT phase (hollow site), and (c) the Na-derived band of the LT phase. The positions of cross sections are indicated in Figs. 4(a) and 4(b). Large dots denote Na atoms and small dots Al atoms. The contours begin at 1.0, and the contour spacing is 1.0. The units are $\times 10^{-3}e$ bohr^{-3}.

atoms, where the density for the free Na layer [see Fig. 5(b)] is much larger than that of the Al surface states [see Fig. 6(a)]. We may thus conclude that the electron transfer occurs from Na atoms directly into the *pre-existing surface states* of Al.

It is noted in passing that this character of the LT phase shows a close analogy to the case of $c(2\times2)$-Cs/W(001),[30,31] both having the $c(2\times2)$ fourfold hollow structure. Although the electronic structure is much more complicated for Cs/W, the essential feature of the charge transfer is the same. Thus the maxima of the $4d$-derived surface states of the clean W(001) surface lie on top of the surface W atoms (see Fig. 7 of Ref. 30). The maxima maintain their form upon Cs adsorption. Charge transfer takes place from Cs to these surface states. Hence this case and ours may be regarded as representatives of the alkali-metal-on metal systems, for which the surface states of the substrate play an essential role.

The upper Na-derived band crosses the Fermi level and is partly occupied, remaining ''metallic.'' In Figs. 6(c) and 7(c), its free-electron-like character can be seen. We see in Figs. 6(b) and 6(c) that the charge density of the Al-derived band lies well below the smeared out density of the Na-derived band, and also below the position of the Na atoms. Thus the traditional picture of a thin metallic film covering an originally metallic substrate remains qualitatively valid. We see below that this is *not* the case for the RT phase.

It is to be noted that the apparently weak influence of the Na adsorption on the Al surface states is limited to the high

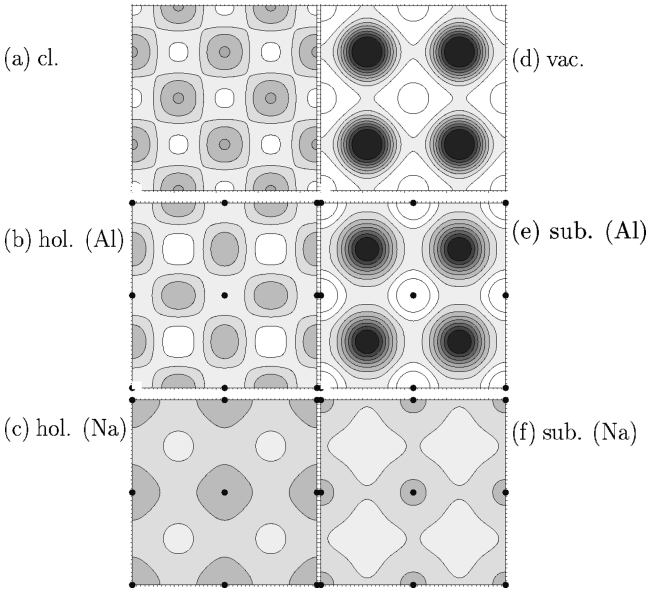

FIG. 7. Charge-density distribution of the main surface states/resonances in a plane parallel to the surface passing through the electron-density maxima (*not* the atom centers): the clean surface (a); the Al- (b) and Na-derived (c) bands of the LT (hollow) structure, respectively; and the vacancy structure (d) and Al- (e) and Na-derived (f) bands of the RT (substitutional) structure, respectively. The dots represent the positions of the Na atoms. The contours begin at 1.0, and the contour spacing is 1.0. The units are $\times 10^{-3}e$ bohr^{-3}.

coverage of $\Theta=0.5$ for the $c(2\times2)$ structure, for which the density maxima for the Na valence electrons [Fig. 5(b)] lie *between* the Na atoms and are situated just at the same site as the surface-state maxima. In fact, it has been found experimentally[10] that at low coverages $\Theta=0$–0.15 the surface states are deteriorated by Na adsorption. Also, it has been shown by DFT calculation[32] for a fictive ordered-structure model $p(2\times2)$, with coverage $\Theta=\frac{1}{4}$, that the surface-state maxima are moved from the on-top sites to the bonding-line positions between the Na and Al atoms.

C. RT $c(2\times2)$ substitutional structure

1. Al-derived band

Figure 2(c) shows the experimental (left panel) and calculated (right panel) surface-state/resonance bands for the RT $c(2\times2)$ substitutional structure. It can be seen that the experimental surface-state/resonance band clearly exhibits a $c(2\times2)$ periodicity, in contrast to the LT (hollow) structure. As we will see below, this is due to the significantly reconstructed Al(001) surface. The calculations (right panel) show good agreement with experiment, and indicate that the band is mainly Al derived (circles), but has a small participation of Na (squares). The energy position of the main theoretical and experimental bands at $\bar{\Gamma}$ are 2.14 and 2.31 eV, respectively.

The experimental results display some asymmetry in the intensity near $\mathbf{k}_{\parallel}=0.5$ in $\bar{\Gamma}$-$\bar{M}$, i.e. a weakening on the left side and a strengthening and upward shift on the right. A few alternative explanations may be possible for this anomaly. Among others, it may be related to the closing of the bulk-band gap in this region, causing the state to go from being a

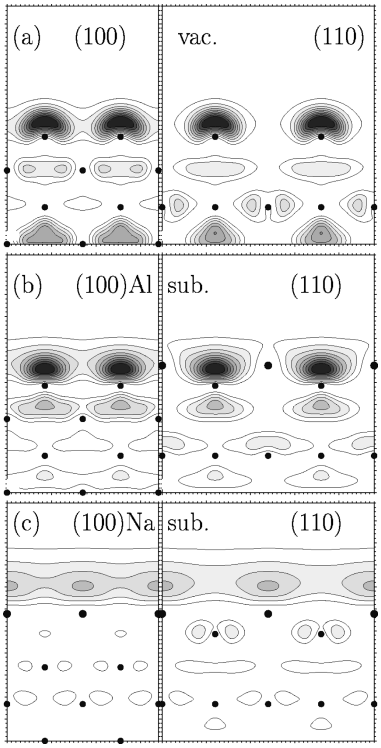

FIG. 8. Same as Fig. 6, for the RT phase (substitutional site). The positions of the cross sections are specified in Figs. 4(c) and 4(d).

pure surface state to a surface resonance [see Fig. 10(c) of Ref. 10]. Also, additional coupling to bulk states may become possible by surface umklapp processes. The peak profile may become broad and complicated, as indicated by the split structure of the band near $\mathbf{k}_{\|}=0.5$ in $\bar{\Gamma}$-$\bar{M}$. Different profiles for the left and right halves may result from this broadened peak in the formation of the matrix element given by Eq. (4), the final state being different.

An important finding in the present analysis is that the main band in the RT structure can be regarded as being derived from the surface-state/resonance band of a fictive, reconstructed clean Al surface, that is, the ''vacancy'' structure; see Fig. 4(c). In this structure the Na atoms are replaced by ''vacancies'' of the Al atoms. The surface-state/resonance band structure of the vacancy structure is displayed in Fig. 3(c). By comparison with Fig. 3(b), it is clearly seen that the main Al-derived band of the RT phase originates from that of the vacancy structure, and is only somewhat shifted down in energy (by 0.81 eV) due to Na adsorption.

Figures 8(a) and 8(b) show the single-state charge distribution at $\bar{\Gamma}$ for the main bands of the ''vacancy structure'' and the RT phase, respectively. Figures 7(d) and 7(e) show their cross sections parallel to the surface passing through the electron-density maxima. Similarly to the clean Al(001) surface, the maxima of charge density for the vacancy structure lie on top of the uppermost surface Al atoms, having this time the $c(2\times2)$ periodicity. For the Al-derived band of the RT phase, the maxima also lie approximately at the same position as that of the vacancy structure, with relatively small changes in their form. It can be noted that these states are rather strongly localized. This explains the well-developed $c(2\times2)$ character of the band found in Fig. 2(c), and its relatively small dispersion (larger value of m^*, see Table II).

Similarly to the LT phase, in Fig. 2(c) we find a few additional theoretical bulk bands which are not present for the clean surface. These are apparently introduced by the $c(2\times2)$ periodicity as surface umklapp processes. There is also indication of a third, relatively weak band lying at E_F and around $\bar{\Gamma}$ and $\bar{M}$ in both the experimental and calculated band structures. From our analysis (not shown), this band can be regarded as being derived from a second, relatively weak, surface-state/resonance band of the vacancy structure.

2. Na-derived band

In Fig. 3(b), we see that the Na-derived band (filled squares) is found only in the calculation, lying completely in the positive-energy range, about 2.7 eV higher in energy than for the free $c(2\times2)$-Na layer. Notably, this shift is much larger than the downward shift of the Al-derived band (0.8 eV). This will be discussed below.

The single-state charge distribution of the unoccupied Na-derived state at $\bar{\Gamma}$ is shown in Fig. 8(c), indicating again an antibonding character. Figures 8(c) and 7(f) show its smeared out, free-electron-like structure, with the maxima residing this time above the Na atoms.

3. Formation mechanism of the two bands

We conclude that the two main bands are resulting, just as in the case of the LT phase, from the coupling between the states of a free $c(2\times2)$-Na monolayer and the surface state/resonance of the Al surface, i.e., the vacancy structure in this case. The electron transfer can also be regarded as occurring from Na atoms into the surface state/resonance of the vacancy structure. This can be seen clearly in comparing Fig. 10 with Fig. 8(a). In the charge redistribution $\Delta\rho_{\text{redis.}}$ in Fig. 10 we note some regions of depletion: the electron charge has been transferred in this case mainly from the region on top of the Na atoms, where the density of the free Na layer dominates the density of the surface state/resonance of the vacancy structure. The charge depletion found in Fig. 10 also near the centers of the Al atoms may be interpreted as a result of an upward shift of the maximum of the surface states induced by Na adsorption.

These findings, combined with the unbalanced large upward shift of the Na-derived band and the existence of the third peak at E_F, both mentioned above, indicate that the coupling between the free Na monolayer states and the Al surface states/resonances takes place in a little more complicated way than in the LT case. It can no longer be interpreted in a simple two-term-coupling perturbation scheme. Apparently the coupling is too strong, and involves other states, namely, the p_z states of Na lying originally at $+1$ eV [Fig. 5(a)] and the second surface states/resonances of Al lying originally at 0 eV [Fig. 3(c)].

We have seen above that for the LT phase the traditional picture of a thin metallic film covering a metallic substrate remains qualitatively valid. For the RT phase, on the other hand, we see in Fig. 8(b) that the completely filled Al-derived band has the maxima lying at the *same* height as the Na atoms. The maxima of the Na-derived band lie indeed

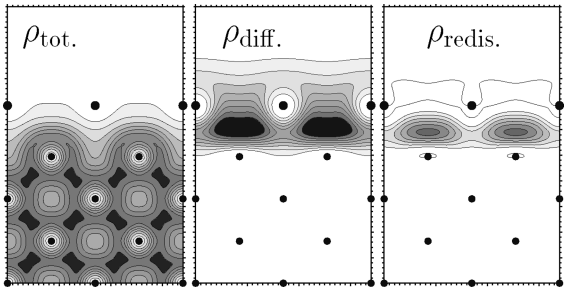

FIG. 9. Total charge-density distribution $\rho_{\mathrm{tot.}}$ (left panel), density difference $\Delta\rho_{\mathrm{diff.}}$ (middle panel), and density redistribution $\Delta\rho_{\mathrm{redis.}}$ (right panel), of the LT phase (hollow site). The cross section is in the (001)Na plane [see Fig. 4(b)]. The units are $10^{-3}e$ bohr^{-3}. In the left panel the first contour begins at 4.0 with a spacing of 4.0; for the middle panel the first contour begins at 0.6 with a spacing of 0.6; and in the right panel the contours are the same as the middle panel, with the addition of a negative contour line (unshaded) at -0.6.

higher, but they are empty. Thus, as far as the electronic states in the energy range near E_F are concerned, the Al-derived band constitutes practically the ''surface'' of this structure. The Na monolayer (or the Na/Al composite monolayer) cannot be regarded as a metallic film on a metallic substrate; rather, except for the still existent background bulk continuum, the electronic structure of the monolayer may be viewed as being analogous to that of an *ionic* crystal, like NaCl, where the completely filled Al-derived band replaces the valence band of Cl, and forms with the empty Na-derived band a ''band gap'' of about 3.5 eV across the Fermi energy.

We note in passing that we find a similarity of the surface electronic structure of the RT phase to that of the system (2×2)-2Na/Al(111) which forms a composite double-layer surface alloy with a similar, but more complex intermixing of Na and Al in the surface layers.[33,34] For this system we find also a filled Al-derived band originating from the corresponding ''vacancy structure,'' and an empty Na-derived band. (The latter may be assigned to that found by Heskett *et al.*[35] using inverse photoemission spectroscopy.) The similarity indicates that also this layer cannot be regarded simply as a thin metallic layer.

V. DISCUSSION

For all three systems studied [Al(001) and the two $c(2\times2)$-Na/Al(001) phases], we find good overall agreement of the surface-state/resonance band structure between experiment and theory. In each case there is a prominent Al-derived surface-state/resonance band, showing similar free-electron-like parabolic dispersion at the band bottom near $\overline{\Gamma}$, as indicated by broken lines in Fig. 2. We find that the observed and calculated values of the Fermi wave vector, $\mathbf{k}_F$ and the effective mass m^* of the main band (Table II) agree only roughly, probably due to the approximations used in calculation, as already mentioned. In any case, these quantities are to be regarded as global parameters specifying only the geometry of the bands, and are not intended to indicate that the bands are free-electron-like. In fact, the wave functions of the Al-derived bands are rather strongly localized, as we see from the charge-density distributions. The dispersion of the bands may be regarded as the result of the overlap between the localized wave functions.

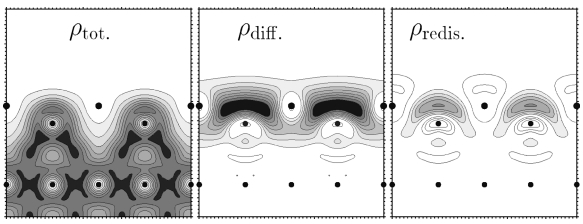

FIG. 10. Same as Fig. 9 for the RT phase (substitutional site). For the middle panel there is one contour line at -1.2, and in the right panel there are three negative contour lines (unshaded) at -1.8, -1.2, and -0.6.

The picture of charge transfer taking place from Na to the surface states/resonances of Al is also supported by the almost equal values of the work-function change (decrease) $\Delta\Phi\approx-1.6$ eV, obtained both experimentally[36,37] and theoretically in the present work for the LT and RT phases. Obviously the value of $\Delta\Phi$ results from $\rho_{\mathrm{redis.}}$, shown in Figs. 9 and 10, as the z component of the dipole moment. As already mentioned, the *minima* and maxima of $\rho_{\mathrm{redis.}}$ correspond to the maxima of the Na- and Al-derived states, respectively. This can be seen by comparison of Figs. 9 and 10 with Figs. 6(b) and 6(c) and 8(b) and 8(c). In these figures, the vertical distances between the maxima of the Na- and Al-derived states are found to have a ratio of about 1.0 to 0.6 between the LT and RT phases. On the other hand, a comparison between Figs. 5(a) and 2(b) shows that the decrease of the occupancy of the Na-derived states amounts to c. 0.6 for the LT phase, in contrast to 1.0 for the RT phase (being empty). This leads to the same amount of $\Delta\Phi$ between the two phases, as a product of charge and distance. It is essential in this consideration to note the fact that, while the forms of the Al-derived states remain always almost unchanged, the forms of the Na-derived states change drastically, from that of Figs. 5(b) to those of Figs. 6(c) and 8(c).

Our results verify the formation of the *two* surface-state/resonance bands. Various experimental methods of studying surface electronic properties other than ultraviolet photoelecton spectroscopy, as used here, may be useful for finding out characteristic features induced by these two bands. Particularly, EELS (electron-energy-loss spectroscopy) (Refs. 38 and 39) and inverse photoemission spectroscopy[35,39] may be useful for studying the effects of the bands lying in the energy range above the Fermi level.

For the RT phase, the fact that the surface band structure is constituted of a filled band and an empty band, with a gap of approximately 3.5 eV, may play an important role in various properties of the surface. We may think of, in addition to EELS, an anomalous feature in optical reflection spectra[40] near 3.5 eV and a corresponding anomaly in the dispersion curve of surface plasmons.[41]

A significant effect may be expected in various surface-sensitive methods, such as ion neutralization,[42] metastable deexcitation,[42,43] etc., which would reflect the dominance of the surface states/resonances in the outermost surface region, and hence expose the difference in the character of these states between the LT and RT phases. We may also think of the relevance of the occupancy of surface states/resonances on surface diffusion[44] and catalytic activity.[45]

VI. CONCLUSION

We have analyzed the electronic structure of the metastable hollow and stable substitutional structures of $c(2\times2)$-Na on Al(001). The calculated surface-state/resonance bands agree well with those measured by angle-resolved photoemission experiments. It is found that, in both phases, two pronounced bands appear as the result of a characteristic coupling between the valence-state bands of a free $c(2\times2)$-Na layer and the surface-state/resonance bands of the corresponding (i.e., clean and reconstructed) Al surfaces. While the experimental band structure of the substitutional structure shows a clear $c(2\times2)$ character due to the significant reconstruction of the surface Al layer, the hollow structure does not: The main band, in fact, exhibits a quasi-(1×1) periodicity like that of the clean surface. For the stable substitutional structure, the unoccupied surface-state/resonance band lies completely above the Fermi level, leading to the formation of a surface-state band structure that resembles that of an ionic crystal. We await experimental verification of the predicted unoccupied surface-state/resonance band, and of the difference in the properties of the LT and RT phases in relation to the character of the surface states/resonances.

[1] C. Stampfl and M. Scheffler, Surf. Rev. Lett. **2**, 317 (1995); J. N. Andersen, *ibid.* **2**, 345 (1995); R. Fasel and J. Osterwalder, *ibid.* **2**, 359 (1995); R. D. Diehl and R. McGrath, *ibid.* **2**, 387 (1995); H. Over, H. Bludau, M. Gierer, and G. Ertl, *ibid.* **2**, 409 (1995).

[2] R. Diehl and R. McGrath, Surf. Sci. Rep. **23**, 43 (1996).

[3] B. Hutchins, T. Rhodin, and J. Demuth, Surf. Sci. **54**, 419 (1976).

[4] M. Van Hove, S. Y. Tong, and N. Stoner, Surf. Sci. **54**, 258 (1976).

[5] J. N. Andersen, E. Lundgren, R. Nyholm, and M. Qvarford, Phys. Rev. B **46**, 12 784 (1992).

[6] S. Aminpirooz, A. Schmalz, L. Becker, N. Pangher, J. Haase, M. M. Nielsen, D. R. Batchelor, E. Bøgh, and D. L. Adams, Phys. Rev. B **46**, 15 594 (1992).

[7] C. Stampfl, J. Neugebauer, and M. Scheffler, Surf. Rev. Lett. **1**, 213 (1994).

[8] W. Berndt, D. Weick, C. Stampfl, A. M. Bradshaw, and M. Scheffler, Surf. Sci. **330**, 182 (1995).

[9] R. Fasel, P. Aebi, J. Osterwalder, L. Schlapbach, R. G. Agostino, and G. Chiarello, Phys. Rev. B **50**, 14 516 (1994).

[10] R. Fasel, Ph.D. thesis, Université de Fribourg, 1996; R. Fasel, P. Aebi, R. G. Agostino, J. Osterwalder, and L. Schlapbach, Phys. Rev. B **54**, 5893 (1996).

[11] J. Osterwalder, P. Aebi, R. Fasel, D. Naumovic, P. Schwaller, T. Kreutz, L. Schlapbach, T. Abukawa, and S. Kono, Surf. Sci. **331-333**, 1002 (1995).

[12] Details about the determination and calibration of Na coverages can be found in Ref. 10.

[13] J. Neugebauer and M. Scheffler, Phys. Rev. B **46**, 16 067 (1992).

[14] R. Stumpf and M. Scheffler, Comput. Phys. Commun. **79**, 447 (1994); M. Bockstedte, A. Kley, J. Neugebauer, and M. Scheffler, Comput. Phys. Commun. **107**, 187 (1997).

[15] R. Hora and M. Scheffler, Phys. Rev. B **29**, 692 (1984).

[16] M. Heinrichsmeyer, A. Fleszar, and A. G. Eguiluz, Surf. Sci. **285**, 129 (1993).

[17] A. P. Seitsonen, B. Hammer, and M. Scheffler (unpublished).

[18] E. V. Chulkov and V. M. Silkin, Surf. Sci. **215**, 385 (1989).

[19] G. Wachutka, Phys. Rev. B **34**, 8512 (1986).

[20] J. E. Inglesfield and G. A. Benesh, Surf. Sci. **200**, 135 (1988); J. Phys. C **19**, 539 (1986).

[21] M. Seel, Phys. Rev. B **28**, 778 (1983).

[22] H. Krakauer, M. Posternak, A. J. Freeman, and D. D. Koelling, Phys. Rev. B **23**, 3859 (1981).

[23] E. Caruthers, L. Kleinman, and G. P. Alldredge, Phys. Rev. B **8**, 4570 (1979).

[24] P. O. Gartland and B. J. Slagsvold, Solid State Commun. **25**, 489 (1978).

[25] G. V. Hansson and S. A. Flodström, Phys. Rev. B **18**, 1562 (1978); **19**, 3329(E) (1979).

[26] S. D. Kevan, N. G. Stoffel, and N. V. Smith, Phys. Rev. B **31**, 1788 (1985).

[27] G. A. Benesh, H. Krakauer, D. E. Ellis, and M. Posternak, Surf. Sci. **104**, 599 (1981); G. A. Benesh and J. R. Hester, *ibid.* **194**, 567 (1988).

[28] C. A. Coulson, *Valence*, 2nd ed. (Oxford University Press, London, 1961), p. 71.

[29] P. W. Atkins, *Molecular Quantum Mechanics*, 2nd ed. (Oxford University Press, London, 1983), p. 25.

[30] E. Wimmer, A. J. Freeman, J. R. Hiskes, and A. M. Karo, Phys. Rev. B **28**, 3074 (1983).

[31] P. Soukiassian, R. Riwan, J. Lecante, E. Wimmer, S. R. Chubb, and A. J. Freeman, Phys. Rev. B **31**, 4911 (1985).

[32] C. Stampfl (unpublished).

[33] C. Stampfl and M. Scheffler, Surf. Sci. **319**, L23 (1994).

[34] J. Burchhardt, M. M. Nielsen, D. L. Adams, E. Lundgren, J. N. Andersen, C. Stampfl, M. Scheffler, A. Schmalz, S. Aminpirooz, and J. Haase, Phys. Rev. Lett. **74**, 1617 (1995).

[35] D. Heskett, K.-H. Frank, K. Horn, E. E. Koch, H.-J. Freund, A. Baddorf, K.-D. Tsuei, and E. W. Plummer, Phys. Rev. B **37**, 10 387 (1988); D. Heskett, K.-H. Frank, E. E. Koch, and H.-J. Freund, *ibid.* **36**, 1276 (1987).

[36] J. O. Porteus, Surf. Sci. **41**, 515 (1974).

[37] J. Paul, J. Vac. Sci. Technol. A **5**, 664 (1987).

[38] T. Aruga and Y. Murata, Prog. Surf. Sci. **31**, 61 (1989).

[39] *Unoccupied Electronic States*, edited by J. C. Fuggle and J. E. Inglesfield (Springer, Berlin, 1992).

[40] J. D. E. McIntyre, in *Optical Properties of Solids, New Developments*, edited by B. O. Seraphin (North-Holland, Amsterdam, 1976), p. 555.

[41] H. Raether, *Surface Plasmons on Smooth and Rough Surfaces and Gratings* (Springer, Berlin 1988).

[42] H. D. Hagstrum, in *Chemistry and Physics of Solid Surfaces VII*, edited by R. Vanselow and R. How (Springer, Berlin, 1988), p. 341.

[43] J. Küppers, in *Physics and Chemistry of Alkali Metal Adsorption*, edited by H. P. Bonzel, A. M. Bradshaw, and G. Ertl (Elsevier, Amsterdam, 1989), p. 45.

[44] E. Bertel, P. Roos, and J. Lehmann, Phys. Rev. B **52**, R14 384 (1995).

[45] N. Memmel and E. Bertel, Phys. Rev. Lett. **75**, 485 (1995).